NEW UNSUPERVISED CLASSIFICATION OF THE MARTIAN SURFACE INTO TES THERMAL-INERTIA ALBEDO UNITS. E. Jones[1,2,3], F. Mills[3,4], B. Doran[3], G. Caprarelli[5], and J. Clarke[2,6]
[1]Research School of Astronomy and Astrophysics, Australian National University, eriita@mso.anu.edu.au; [2]Mars Society Australia Inc.; [3]Fenner School of Environment and Society, Australian National University; [4]Research School of Physics and Engineering, Australian National University; [5]Department of Environmental Sciences, University of Technology Sydney; [6]Australian Centre for Astrobiology, Macquarie University.

Introduction: Maps of thermal inertia – albedo units have been demonstrated to provide information on the distribution of surface materials on Mars [1,2]. Previous work has used deterministic methods to threshold the dominant values in thermal inertia and albedo from the Thermal Emission Spectrometer (TES), producing a map of 7 thermo-physical units [2]. The units were interpreted as mixtures in various proportions of three principal surface components: dust, bedrock and ice. The use of deterministic methods to define threshold captures important information from the thermal inertia and albedo data but discards potentially significant patterns and can introduce biases. An alternative is to use unsupervised classification algorithms. We have utilized unsupervised classification algorithms to identify Martian surface features, at multiple cluster resolutions. The classification algorithms are not biased towards the most distinctive thermal inertia and albedo information and hence, they reveal substantial structure in medium - high thermal inertia materials that were not seen in previous works. In this study we present and interpret results for 7 [3] and 10 [4] thermo-physical units on the Martian surface in TES thermal inertia and albedo data at 1/20˚ resolution.

Methods: Unsupervised classification is broadly used in the interpretation of terrestrial remote sensing and involves using a clustering algorithm to group pixels that have similar values in each measurement parameter. The algorithms used in this study were isodata for training and maximum likelihood for classification. For a specified number of clusters, N, isodata defines N training clusters by seeding N cluster centers equally spaced across the parameter space and then assigning pixels to a cluster if the parameter distance between the pixel and the cluster centre is less than the distance to all other cluster centers. Each cluster centre is then recalculated as the mean of the pixels assigned to the cluster. This process of assigning pixels and recalculating cluster means is continued iteratively until either the maximum number of iterations is reached or the pixels assignment is changing little between successive iterations [5]. The statistical parameters of the N training clusters are then fed into the classification algorithm. Maximum likelihood assumes that the distribution of each of the N clusters will be multivariate normal and then assigns pixels to the cluster to which they have the highest probability of belonging [6]. The validity of the clustering can be quan-

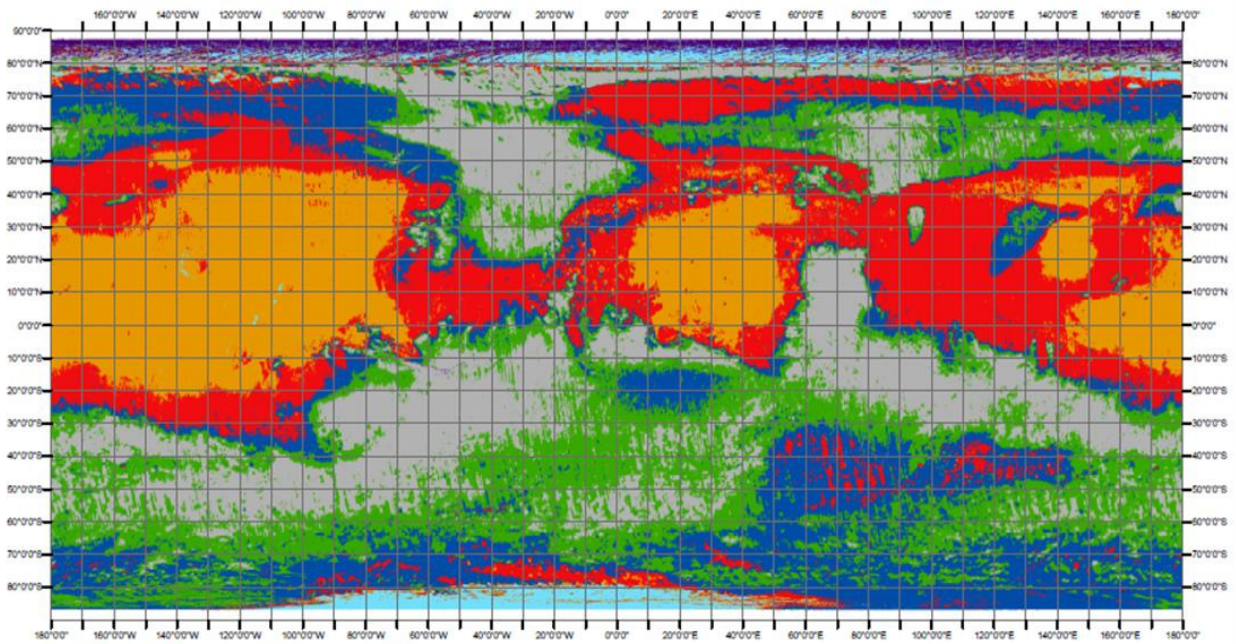

Figure 1. Map of the Martian surface classified into 7 thermo-physical clusters [3]. The key is given in Table 1.

tified through a χ^2 distribution with degrees of freedom equal to the number of input parameters [7]. The clusters are then mapped and interpreted as mixtures of dust, sand, duricrust, bedrock and ice on the Martian surface through comparing the cluster's distribution of thermal inertia and albedo to the known behaviour of different grain sizes on Mars (eg. [8-11]). In our initial study [3] unsupervised cclassification algorithms were used to find 7 distinct clusters in the data, so that a direct comparison with the 7 clusters defined in [2] could be undertaken. We have also expanded the classification to define 10 clusters [4], providing higher resolution in the distribution of surface materials than N=7 and more coherent special patterning than N>10.

Results: A pattern of global 'enveloping' can be seen in the spatial occurrence of the clusters, mirrored on either side of the equator in both the 7 cluster (Fig. 1) and 10 cluster maps [4]. This corresponds to a decrease in albedo with increasing distance from the equator through the sequence of clusters. The mean thermal inertia also generally increases through this sequence.

The results of the 7 cluster study agree with [2] in the equatorial region where bright fines dominate. However, the unsupervised classification map provides evidence of additional structure in the distribution of surface materials at higher latitudes, particularly in areas of low albedo and moderate-high thermal inertia such as Acidalia and Sinus Meridiani. Cluster 4 (Figure 1, Table 1) is very similar to class C in [2] however it is spatially associated with cluster 3 which was not differentiated in [2]. Furthermore, clusters 1 and 2 are not differentiated in [2] as they were incorporated into class B.

The results of the 10 cluster study closely agree with [2] and [3] in both the equatorial region where bright fines dominate, and in the locations of the darkest low thermal inertia materials. The closest agreement between the 10 cluster map [4] and Fig. 5 in [2] occurs in clusters 8 and 1. Cluster 8 is consistent with a > 2 cm thick layer of bright dust grains < 10 µm across and has 68% agreement with class A in [2]. Cluster 1 shows 96% agreement with class E in [2]. It has extremely low albedo and is consistent with a surface that is predominately sand and small rocks < 4 cm across. We find that cluster 1 may also contain some shallow ice-cemented soil in the northern polar terrain and possibly at lower latitudes (consistent with detections of low-latitude surface water frost, [12,13]). Cluster 9, which is consistent with ice, ice-cemented soil, and/or large rocks/bedrock up to 2 m across under a thin coating of bright dust, is present at both poles. This cluster is not fully identified in [2] and falls into Classes A and G. The remaining clusters in our study are interpreted as varying ratios of bright dust and darker, coarser grains.

These maps provide important insights into how past fluvial and aeolian processes have distributed materials and sorted grain sizes on the Martian surface. For example, the Valles Marineris canyon system is clearly detailed in cluster maps with the boundaries between different clusters closely matching the boundaries between several distinct geologic units. The coherent spatial patterning in cluster maps, and the correlation with some geologic features, known shallow ice, and the global dust cover index, indicates is the cluster maps are sensitive to real trends in surface materials. Detailed analysis and comparison to the mineralogy and geologic context of each cluster is underway.

Table 1: Interpretation of 7 thermo-physical units from [3]

Cluster	Interpretation
1	Duricrust, rocks, sand
2	Duricrust, sand
3	Duricrust, sand, dark fines
4	Duricrust, sand, dust
5	Dust
6	Ice
7	Ice, rocks

References: [1] Mellon, M.T. et al. (2000) *Icarus, 148,* 437; [2] Putzig, N.T. et al. (2005) *Icarus, 173,* 325; [3] Jones, E.G., et al. *ASSC Proceedings* (submitted 2010); [4] Jones, E.G., et al. *J. Geophys. Res.* (submitting in February 2011); [5] Ball, G.H. and Hall, D.J. (1965) *Stanford Research Institute*, California; [6] Duda, R.O and Hart, P.E. (1973) *Wiley Publishers,* New Jersey; [7] Swain, P.H. (1973) *McGraw-Hill International,* Sheffield; [8] Christensen, P.R. (1986) *J. Geophys. Res., 91,* 3533; [9] Jakosky, B.M. (1986) *Icarus., 66*, 117; [10] Jakosky, B.M. and Christensen, P.R. (1986) *J. Geophys. Res., 91*, 3547; [11] Presley, M.A. and Christensen, P.R. (1997) *J. Geophys. Res., 102,* 6551; [12] Carrozzo, F.G., et al. (2009) *Icarus, 203,* 406; [13] Vincendon, M., et al. (2010) *J. Geophys. Res., 115,* E003584